On the energy contribution of explicit time-integration in projection methods

J. Plana-Riu, S.M. Šehović, F.X. Trias, A. Oliva

Heat and Mass Transfer Technological Centre
Technical University of Catalonia

15th ERCOFTAC Workshop on Direct & Large Eddy Simulation
Delft, the Netherlands
May 10th, 2026

Introduction

Energy conservation in Computational Fluid Dynamics

Lots of efforts have been made to design energy-conserving spatial discretizations:

- Piacsek & Williams (1970): skew-symmetric formulation of the convective term.
- Verstappen & Veldman (2003): shift the focus to fundamental mimetic properties of the discrete operators in staggered grids.
- Trias et al. (2014): extend the concept to collocated grids.

But what about the time-integration scheme?

Energy-conservation in time-integration

Symplectic integration schemes

By definition, symplectic methods are those designed to guarantee the conservation of the symplectic form, which is a geometric structure that encodes the energy of the system.

- They are widely used in Hamiltonian systems, such as celestial mechanics and molecular dynamics.
- They are designed to preserve the energy of the system over long time periods, which is crucial for accurate simulations.
- However, they are **fully implicit**, which makes them computationally expensive and not suitable for large-scale CFD simulations.

Some explicit methods can be constructed to be pseudo-symplectic: preservation of energy up to a certain order of accuracy, but they are not fully symplectic and may not guarantee long-term energy conservation.

Projection methods

Saddle-point formulation of the Navier-Stokes equations

$$\begin{bmatrix} \mathcal{A}(\mathbf{u}_h^{n+1}) & G \\ M & 0 \end{bmatrix} \begin{bmatrix} \mathbf{u}_h^{n+1} \\ \mathbf{p}_h^{n+1} \end{bmatrix} = \begin{bmatrix} \mathbf{r}_h^{n+1} \\ \mathbf{g}_h^{n+1} \end{bmatrix} + \begin{bmatrix} \Delta t^{-1} I & 0 \\ 0 & 0 \end{bmatrix} \begin{bmatrix} \mathbf{u}_h^{n} \\ \mathbf{p}_n^{n} \end{bmatrix}$$

First introduced by Chorin (1968) and Temam (1969), they decouple the pressure and velocity fields: splitting error! By applying Perot's LU decomposition:

$$\begin{bmatrix} \mathcal{A}(\mathbf{u}_h^{n+1}) & G \\ M & 0 \end{bmatrix} = \begin{bmatrix} \mathcal{A}(\mathbf{u}_h^{n+1}) & 0 \\ M & -MG\mathcal{A}(\mathbf{u}_h^{n+1})^{-1}G \end{bmatrix} \begin{bmatrix} I & \mathcal{A}(\mathbf{u}_h^{n+1})^{-1}G \\ 0 & I \end{bmatrix}$$

Projection methods

Saddle-point formulation of the Navier-Stokes equations

$$\begin{bmatrix} \mathcal{A}(\mathbf{u}_h^{n+1}) & G \\ M & 0 \end{bmatrix} \begin{bmatrix} \mathbf{u}_h^{n+1} \\ \mathbf{p}_h^{n+1} \end{bmatrix} = \begin{bmatrix} \mathbf{r}_h^{n+1} \\ \mathbf{g}_h^{n+1} \end{bmatrix} + \begin{bmatrix} \Delta t^{-1} I & 0 \\ 0 & 0 \end{bmatrix} \begin{bmatrix} \mathbf{u}_h^{n} \\ \mathbf{p}_n^{n} \end{bmatrix}$$

First introduced by Chorin (1968) and Temam (1969), they decouple the pressure and velocity fields: splitting error! By applying Perot's LU decomposition:

$$\begin{bmatrix} \mathcal{A} & G \\ M & 0 \end{bmatrix} = \begin{bmatrix} \mathcal{A} & 0 \\ M & -\Delta t M G \end{bmatrix} \begin{bmatrix} I & \Delta t G \\ 0 & I \end{bmatrix}$$

Projection methods

Saddle-point formulation of the Navier-Stokes equations

$$\begin{bmatrix} \mathcal{A}(\mathbf{u}_h^{n+1}) & G \\ M & 0 \end{bmatrix} \begin{bmatrix} \mathbf{u}_h^{n+1} \\ \mathbf{p}_h^{n+1} \end{bmatrix} = \begin{bmatrix} \mathbf{r}_h^{n+1} \\ \mathbf{g}_h^{n+1} \end{bmatrix} + \begin{bmatrix} \Delta t^{-1} I & 0 \\ 0 & 0 \end{bmatrix} \begin{bmatrix} \mathbf{u}_h^{n} \\ \mathbf{p}_n^{n} \end{bmatrix}$$

First introduced by Chorin (1968) and Temam (1969), they decouple the pressure and velocity fields: splitting error! By applying Perot's LU decomposition:

$$\begin{bmatrix} \mathcal{A} & G \\ M & 0 \end{bmatrix} = \begin{bmatrix} \mathcal{A} & 0 \\ M & -\Delta t M G \end{bmatrix} \begin{bmatrix} I & \Delta t G \\ 0 & I \end{bmatrix}$$

$$\begin{bmatrix} \Delta t^{-1} & 0 \\ M & -\Delta t M G \end{bmatrix} \begin{bmatrix} \mathbf{u}_h^{*} \\ \mathbf{p}_h^{n+1} \end{bmatrix} = \begin{bmatrix} \mathbf{r}_h^{n+1} + \Delta t^{-1} \mathbf{u}_h^{n} \\ \mathbf{g}_h^{n+1} \end{bmatrix}$$

$$\begin{bmatrix} I & \Delta t G \\ 0 & I \end{bmatrix} \begin{bmatrix} \mathbf{u}_h^{n+1} \\ \mathbf{p}_h^{n+1} \end{bmatrix} = \begin{bmatrix} \mathbf{u}_h^{*} \\ \mathbf{p}_h^{n+1} \end{bmatrix}$$

Projection methods

Saddle-point formulation of the Navier-Stokes equations

$$\begin{bmatrix} \mathcal{A}(\mathbf{u}_h^{n+1}) & G \\ M & 0 \end{bmatrix} \begin{bmatrix} \mathbf{u}_h^{n+1} \\ \mathbf{p}_h^{n+1} \end{bmatrix} = \begin{bmatrix} \mathbf{r}_h^{n+1} \\ \mathbf{g}_h^{n+1} \end{bmatrix} + \begin{bmatrix} \Delta t^{-1} I & 0 \\ 0 & 0 \end{bmatrix} \begin{bmatrix} \mathbf{u}_h^{n} \\ \mathbf{p}_n^{n} \end{bmatrix}$$

First introduced by Chorin (1968) and Temam (1969), they decouple the pressure and velocity fields: splitting error! By applying Perot's LU decomposition:

$$\begin{bmatrix} \mathcal{A} & G \\ M & 0 \end{bmatrix} = \begin{bmatrix} \mathcal{A} & 0 \\ M & -\Delta t M G \end{bmatrix} \begin{bmatrix} I & \Delta t G \\ 0 & I \end{bmatrix}$$

Standard projection method

$$\begin{aligned} \mathbf{u}_h^* &= \mathbf{u}_h^n + \Delta t \mathbf{r}_h^{n+1} \\ L\overline{\mathbf{p}}_h^{n+1} &= M\mathbf{u}_h^* - \mathbf{g}_h^{n+1} \\ \mathbf{u}_h^{n+1} &= \mathbf{u}_h^* - G\overline{\mathbf{p}}_h^{n+1} \end{aligned}$$

Projection method with pressure correction

$$\begin{aligned} \mathbf{u}_h^* &= \mathbf{u}_h^n + \Delta t \mathbf{r}_h^{n+1} - G\overline{\mathbf{p}}_h^n \\ L\overline{\phi}_h^{n+1} &= M\mathbf{u}_h^* - \mathbf{g}_h^{n+1} \\ \mathbf{u}_h^{n+1} &= \mathbf{u}_h^* - G\overline{\phi}_h^{n+1} \end{aligned}$$

Decision pipeline for time integration

Four main criteria to consider when choosing a time-integration scheme for projection methods:

1. Order of accuracy
2. Stability properties
3. Computational efficiency
4. *Energy conservation properties*

Decision pipeline for time integration

Presence of splitting error

Reconstructing the original monolithic system

$$\mathcal{K}' = \begin{bmatrix} \mathcal{A} & \mathcal{A}\tilde{\mathcal{A}}^{-1}G \\ M & 0 \end{bmatrix}$$

$$\mathbf{e} = (\mathcal{K} - \mathcal{K}') \begin{bmatrix} \mathbf{u}_h^{n+1} \\ \mathbf{p}_h^{n+1} \end{bmatrix} = \begin{bmatrix} 0 & (I - \mathcal{A}\tilde{\mathcal{A}}^{-1})G \\ 0 & 0 \end{bmatrix} \begin{bmatrix} \mathbf{u}_h^{n+1} \\ \mathbf{p}_h^{n+1} \end{bmatrix} = \begin{bmatrix} (I - \mathcal{A}\tilde{\mathcal{A}}^{-1})G\mathbf{p}_h^{n+1} \\ 0 \end{bmatrix}$$

- For the classical projection: $||\mathbf{e}||_2 = (I - \Delta t I)||G\mathbf{p}_h^{n+1}||_2 = \mathcal{O}(\Delta t)$
- With pressure correction: $||\mathbf{e}||_2 = (I - \Delta t I)||G(\mathbf{p}_h^{n+1} - \mathbf{p}_h^n)||_2 = \mathcal{O}(\Delta t^2)$

Splitting error and order of accuracy

Main source of error in projection methods $\rightarrow$ it limits the order of accuracy of the method.

Decision pipeline for time integration

Based on order of accuracy

No need to use higher-order methods (RK3, RK4, etc.) over lower-order ones (Euler, RK2, AB2): **these methods are cheaper and same order of accuracy**.

Why don't we use them then?

Decision pipeline for time integration

Based on order of accuracy

No need to use higher-order methods (RK3, RK4, etc.) over lower-order ones (Euler, RK2, AB2): **these methods are cheaper and same order of accuracy**.

Why don't we use them then?

Stability properties

- Explicit integration: limited by the situation of the eigenvalue of the system in the complex plane.
- Higher-order methods $\rightarrow$ bigger stability region $\rightarrow$ larger time steps $\rightarrow$ more efficient.

Decision pipeline for time integration

Based on order of accuracy

No need to use higher-order methods (RK3, RK4, etc.) over lower-order ones (Euler, RK2, AB2): **these methods are cheaper and same order of accuracy**.

Why don't we use them then?

Stability properties

- Explicit integration: limited by the situation of the eigenvalue of the system in the complex plane.
- Higher-order methods $\rightarrow$ bigger stability region $\rightarrow$ larger time steps $\rightarrow$ more efficient.

- Methods like `EigenCD` or `AlgEigCD` allow to compute the eigenvalues of the system and maximize the time step while ensuring stability.

Decision pipeline for time integration

Stability properties

- Multistage methods (RK2, RK3, RK4) have larger stability regions than multistep methods (AB2-like schemes).
- This allows for larger time steps while maintaining stability.

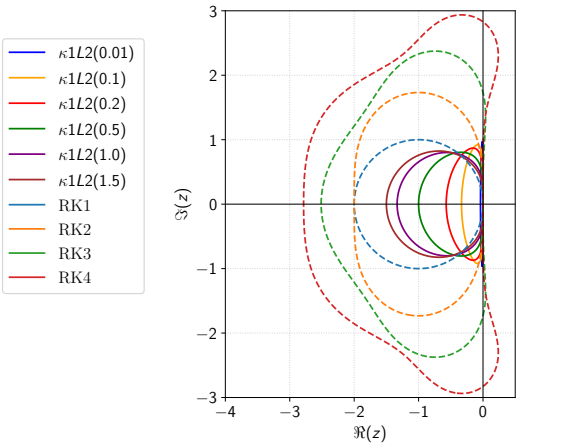

Decision pipeline for time integration

Computational efficiency

Projection methods for Runge-Kutta methods

$$\mathbf{U}_i^* = \mathbf{u}_h^n + \Delta t \sum_{j=1}^{s} a_{ij}\mathbf{F}_j \qquad \mathbf{u}^* = \mathbf{u}_h^n + \Delta t \sum_{j=1}^{s} b_j\mathbf{F}_j$$

$$L\overline{\mathbf{p}}_i = M\mathbf{U}_i^* - \mathbf{g}_i \qquad L\overline{\mathbf{p}} = M\mathbf{u}^* - \mathbf{g}$$

$$\mathbf{U}_i = \mathbf{U}_i^* - G\overline{\mathbf{p}}_i \qquad \mathbf{u}_h^{n+1} = \mathbf{u}^* - G\overline{\mathbf{p}}$$

Decision pipeline for time integration

Projection methods for Runge-Kutta methods

$$\mathbf{U}_i^* = \mathbf{u}_h^n + \Delta t \sum_{j=1}^{s} a_{ij}\mathbf{F}_j \qquad \mathbf{u}^* = \mathbf{u}_h^n + \Delta t \sum_{j=1}^{s} b_j\mathbf{F}_j$$

$$L\bar{\mathbf{p}}_i = M\mathbf{U}_i^* - \mathbf{g}_i \qquad L\bar{\mathbf{p}} = M\mathbf{u}^* - \mathbf{g}$$

$$\mathbf{U}_i = \mathbf{U}_i^* - G\bar{\mathbf{p}}_i \qquad \mathbf{u}_h^{n+1} = \mathbf{u}^* - G\bar{\mathbf{p}}$$

- For an s-stage RK method, we need to solve s Pressure Poisson equations per time step, which can be computationally expensive: *addressed by Fast Projection Methods (De Michele et al. (2020), Karam and Saad (2023), Eid et al. (2025))*.
- For AB2-like methods, only one Poisson equation per time step is needed, which can be more efficient for large-scale simulations.
- Efficiency-wise: Forward Euler is the most efficient method (in terms of how fast we advance in time). Why does no one use it then?

Decision pipeline for time integration

Global kinetic energy balance

$$\frac{E^{n+1} - E^n}{\Delta t} = \text{Convective} + \text{Diffusive} + \text{Pressure} + \text{Source} + \text{Temporal}$$

- Convective term: skew-symmetric formulation $\rightarrow$ energy-conserving spatial discretization.
- Diffusive term: always dissipative.
- Pressure term: zero contribution to the kinetic energy balance if $\nabla \cdot \mathbf{u} = 0$ is satisfied and $M = G^T$.
- Source term: can be either energy-conserving or energy-dissipating, depending on the nature of the source.

Decision pipeline for time integration

Global kinetic energy balance

$$\frac{E^{n+1} - E^n}{\Delta t} = \text{Convective} + \text{Diffusive} + \text{Pressure} + \text{Source} + \text{Temporal}$$

- Convective term: skew-symmetric formulation $\rightarrow$ energy-conserving spatial discretization.
- Diffusive term: always dissipative.
- Pressure term: zero contribution to the kinetic energy balance if $\nabla \cdot \mathbf{u} = 0$ is satisfied and $M = G^T$.
- Source term: can be either energy-conserving or energy-dissipating, depending on the nature of the source.

Temporal error term

It can lead to unphysical energy growth or decay, which can affect the accuracy and stability of the simulation.

Decision pipeline for time integration

Starting from the reduced-index DAE system:

$$\frac{d\mathbf{u}_h}{dt} = P\mathbf{F}(\mathbf{u}_h) + GL^{-1}\mathbf{g}$$

where $P = I - GL^{-1}M$ is the projection operator.

Energy budgets for multistep methods

$$||\mathbf{u}_h^{n+1}||_2^2 = ||\mathbf{u}_h^n||_2^2 + 2\Delta t \sum_{i=0}^{k} \beta_i \langle \mathbf{u}_h^n, P\mathbf{F}(\mathbf{u}_h^{n-i})\rangle + \Delta t^2 \sum_{i,j=0}^{k} \beta_i\beta_j \langle P\mathbf{F}(\mathbf{u}_h^{n-i}), P\mathbf{F}(\mathbf{u}_h^{n-j})\rangle$$

Decision pipeline for time integration

Starting from the reduced-index DAE system:

$$\frac{d\mathbf{u}_h}{dt} = P\mathbf{F}(\mathbf{u}_h) + GL^{-1}\mathbf{g}$$

where $P = I - GL^{-1}M$ is the projection operator.

Energy budgets for multistage methods

$$||\mathbf{u}_h^{n+1}||_2^2 = ||\mathbf{u}_h^n||_2^2 + 2\Delta t \sum_{i=1}^{s} b_i \langle \mathbf{U}_i, P\mathbf{F}(\mathbf{U}_i)\rangle + \Delta t^2 \sum_{i,j=1}^{s} (b_i b_j - b_i a_{ij} - b_j a_{ji}) \langle P\mathbf{F}(\mathbf{U}_i), P\mathbf{F}(\mathbf{U}_j)\rangle$$

Numerical results

Key concept: effective viscosity

- The temporal error term can be interpreted as an effective viscosity, which can be either positive (dissipative) or negative (anti-dissipative).
- This effective viscosity can significantly affect the energy balance of the system, leading to unphysical energy growth or decay.

By definition,

$$\frac{\nu}{\nu^*} = \frac{(E^{n+1} - E^n)/\Delta t - \text{Sources}}{\text{Diffusive}}$$

- For multistep methods, $\text{Diffusive} = \langle \mathbf{u}_h^n, P\mathbf{D}\mathbf{u}_h^n \rangle$.
- For multistage methods, $\text{Diffusive} = \sum_{i=1}^{s} b_i \langle \mathbf{U}_i, P\mathbf{D}\mathbf{U}_i \rangle$.

Numerical results

Taylor-Green vortex

Simulation setup

- 3D Taylor-Green vortex at $\mathrm{Re} = 1600$.
- Collocated grid, finite-volume symmetry-preserving spatial discretization.
- 64^3 grid points, periodic boundary conditions.
- Time step: $\Delta t = 0.001$.
- Integration time: $t \in [0, 20]$.

Numerical results

Taylor-Green vortex

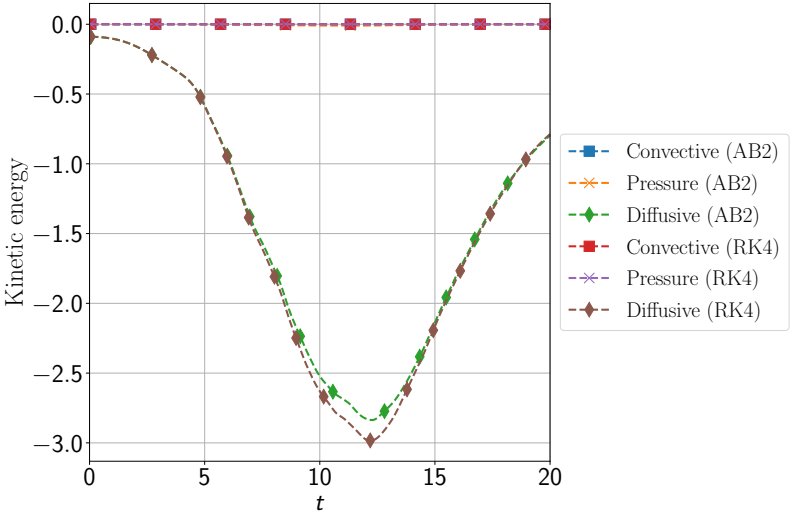

Numerical results

Taylor-Green vortex

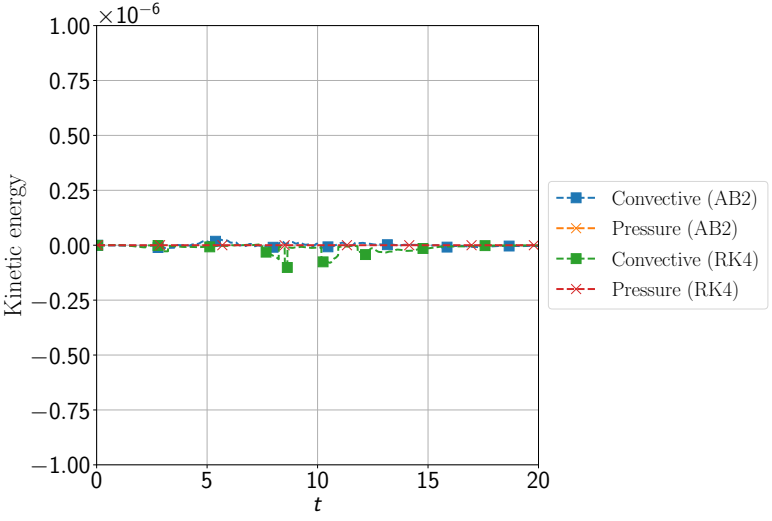

Numerical results

Taylor-Green vortex

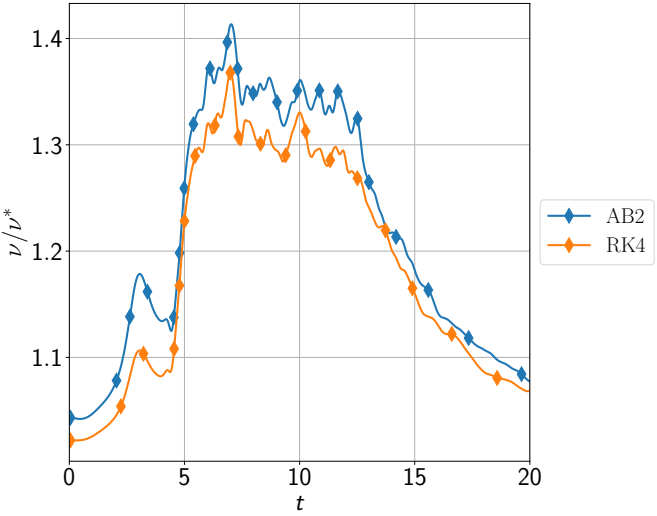

Numerical results

Differentially Heated Cavity

Simulation setup

- *2D* Differentially Heated Cavity of aspect ratio 4 at $\mathrm{Ra} = 6.4 \times 10^8$ and $\mathrm{Pr} = 0.71$.
- Collocated grid, finite-volume symmetry-preserving spatial discretization.
- $128 \times 156 \times 3$ grid points, periodic boundary conditions.
- Time step: $\Delta t = 5 \times 10^{-4}$ (AB2), 1×10^{-3} (RK4).
- Integration time: $t \in [0, 20]$.

Numerical results

Differentially Heated Cavity

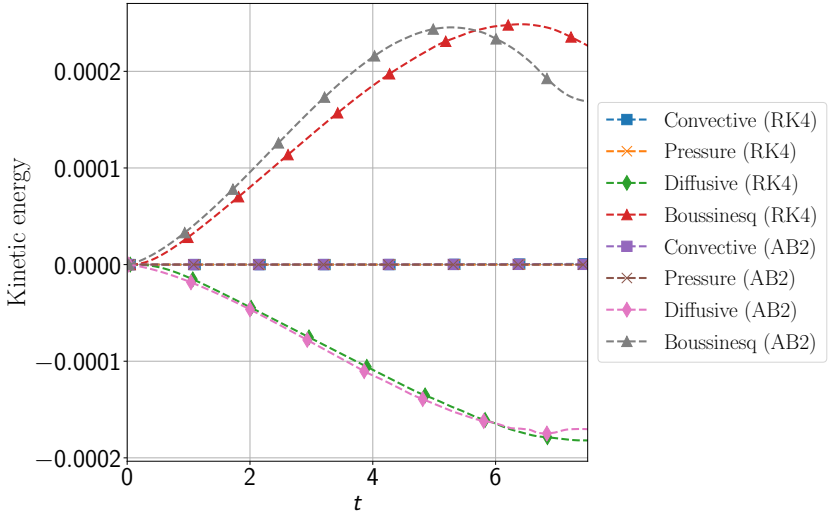

Numerical results

Differentially Heated Cavity

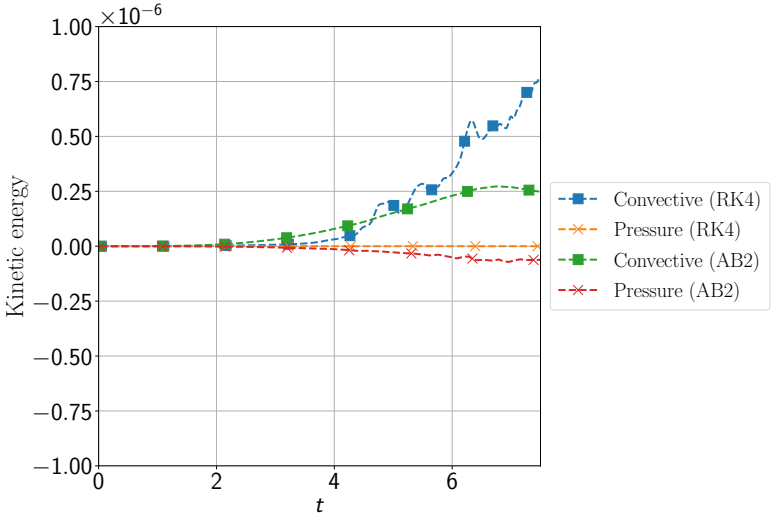

Numerical results

Differentially Heated Cavity

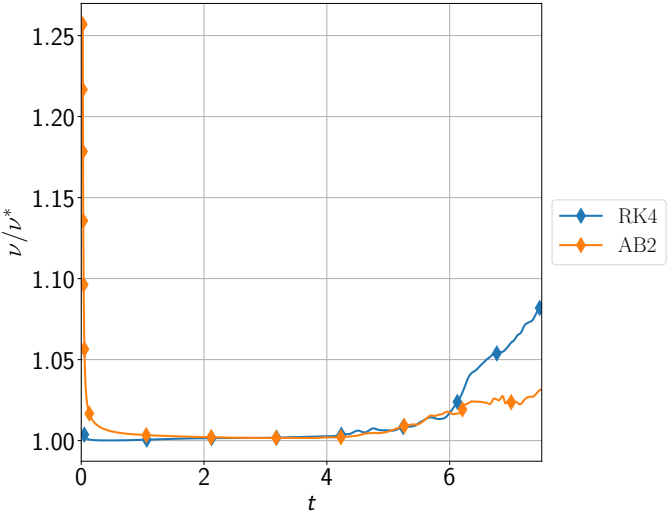

Numerical results

Differentially Heated Cavity: variable Δt

What if Δt is not constant?

- Test for the same geometry
- Using maximum allowed Δt according to `AlgEigCD`
- Schemes: Euler, RK2, RK3, RK4

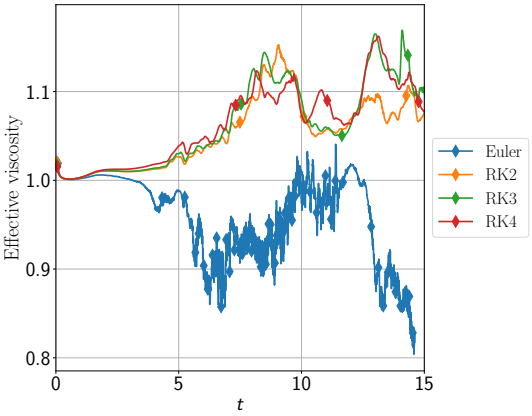

Conclusions

- We have analyzed the pipeline for selecting a time-integration scheme for projection methods, considering order of accuracy, stability properties, computational efficiency, and energy conservation properties.
- We have derived the energy budgets for both multistep and multistage methods, highlighting the contribution of the temporal error term to the kinetic energy balance.
- We have introduced the concept of effective viscosity to interpret the impact of the temporal error term on the energy balance, and we have shown that it can lead to unphysical energy growth or decay.
- We have presented numerical results for the Taylor-Green vortex and the differentially heated cavity, demonstrating the impact of the temporal error term on the energy balance and the effective viscosity.

Future work

There is still a lot of work to be done in this area:

In terms of energy budget analysis

- Implementation of local energy budgets to analyze the spatial distribution of the temporal error term and its impact on the flow dynamics.
- Extension of the analysis to IMEX methods, which are widely used in CFD simulations and can have different energy conservation properties compared to explicit methods.

In terms of tackling energy conservation issues

- Extension of the concept of relaxation Runge-Kutta methods (Ketcheson (2019)) to projection methods, which can help to mitigate the energy conservation issues associated with explicit time-integration schemes.
- Development of new time-integration schemes that are specifically designed to be energy-conserving for projection methods, which can help to improve the accuracy and stability of CFD simulations.

Acknowledgements

The work presented in this conference is supported by the *Ministerio de Economía y Competitividad*, Spain, SIMEX project (PID2022-142174OB-I00).
J.P-R. is supported by a *FI AGAUR-Generalitat de Catalunya* fellowship (2022 FI_B 00810) from the Catalan Agency for Management of University and Research Grants (AGAUR).
S.M.Š. is supported by the *Ministerio de Economía y Competitividad*, Spain, MULTITHERM II project (PID2023-153281OB-I00) with a doctoral grant (PREP223-001454).